Rotational spectrum of 3-aminopropionitrile and searches for it in Sagittarius B2(N)

C Richard, A Belloche, L Margulès, R A Motiyenko, K M Menten, R T Garrod, H S P Müller

Rotational spectrum of 3-aminopropionitrile and searches for it in Sagittarius B2(N)

C. Richard[a,b], A. Belloche[c], L. Margulès[a], R. A. Motiyenko[a], K. M. Menten[c], R. T. Garrod[d] and H. S. P. Müller[e]

[a] *Univ. Lille, CNRS, UMR 8523 - PhLAM - Physique des Lasers Atomes et Molcules, F-59000 Lille, France.*

[b] *Laboratoire Interdisciplinaire Carnot de Bourgogne, UMR 6303 CNRS - Université Bourgogne Franche-Comté, 9 Av. A. Savary, BP 47870, F-21078 Dijon Cedex, France*

[c] *Max-Plank-Institut für Radioastronomie, Auf dem Hügel 69, 53121 Bonn, Germany*

[d] *Departments of Chemistry and Astronomy, University of Virginia, Charlottesville, VA 22904, USA*

[e] *I. Physikalisches Institut, Universität zu Köln, Zülpicher Str. 77, 50937 Köln, Germany*

Abstract

Aminoacetonitrile (NH_2CH_2CN) was detected in the interstellar medium (ISM) one decade ago in the course of a spectral survey of the hot molecular core Sagittarius (Sgr) B2(N) with the IRAM 30 m telescope. With the advent of sensitive telescopes such as the Atacama Large Millimeter/submillimeter Array (ALMA), the degree of chemical complexity in the ISM can be further explored. In the family of aminoacetonitrile, the next stage in complexity with one additional CH_2 group is aminopropionitrile. This molecule has two structural isomers, a chain-like (3-aminopropionitrile, $NH_2CH_2CH_2CN$) and a branched, chiral one (2-aminopropionitrile, $CH_3CH(NH_2)CN$). The latter was studied in the laboratory a few years ago and was not detected in the IRAM 30 m survey. We present the search for both isomers in the EMoCA (Exploring Molecular Complexity with ALMA) survey, a sensitive spectral survey of Sgr B2(N) performed with ALMA. The rotational spectrum of 3-aminopropionitrile has been recorded in laboratory with a submillimeter spectrometer using solid-state sources. Helped by ab-initio calculations performed for the different possible conformations, we present here the analysis based on a Watson Hamiltonian for an asymmetric one-

top rotor in A-reduction performed in the frequency range 150–500 GHz for two conformers. More than 6200 lines of the ground-state and lowest excited vibrational states, corresponding to more than 8200 transitions, were assigned in the experimental spectrum. Partition functions, including the vibrational contribution of these states, and predictions in the JPL-CDMS catalog format were determined in order to search for both conformers of 3-aminopropionitrile in Sgr B2(N). Neither 3-aminopropionitrile, nor 2-aminopropionitrile are detected. The derived upper limits imply that they are at least 12 and 5 times less abundant than aminoacetonitrile, respectively. A comparison to ethyl cyanide and n-propyl cyanide detected in this source suggests that an improvement by a factor three in sensitivity may be sufficient to detect 3-aminopropionitrile, which should be within the range of our on-going follow-up project with ALMA.

Keywords: aminopropionitrile, line identification, molecular data, submillimeter, Sagittarius B2, astrochemistry

1. Introduction

So far (2017), approximately 200 molecules have been detected in the interstellar medium (ISM)[1]. These molecules are mainly composed of the most common atoms present in space: hydrogen, carbon, nitrogen and oxygen. Furthermore, molecules containing a nitrile group at an extremity possess a high dipole moment (see recent examples in Møllendal et al. [1], Richard et al. [2]), allowing possibly an easier detection. A decade ago, Belloche et al. [3] [4] reported the first detection of aminoacetonitrile, NH_2CH_2CN, toward the hot core Sgr B2(N), a high-mass star forming source located close to the Galactic Center. Like many of the most complex organic molecules detected toward this and other chemically-rich sources, the excitation temperature of aminoacetonitrile was determined to be greater than the $\approx$ 100 K beyond which the icy mantles

[1] See, e.g., http://www.nist.gov/pml/data/micro/index.cfm and http://www.astro.uni-koeln.de/cdms/molecules

of dust grains are released into the gas phase; this, combined with its large abundance, suggests that its presence in the gas phase is related to the release of the mantles. Chemical kinetics models by Belloche et al. [5] suggest that aminoacetonitrile can be formed through photochemistry in the dust-grain ice mantles, prior to their ejection into the gas.

Up to now, no molecules with a number of atoms greater than 13 were detected in the interstellar medium or circumstellar shells, except for fullerenes C_{70}, C_{60} and C_{60}^+ [6, 7, 8, 9]. 3-aminopropionitrile ($NH_2CH_2CH_2CN$) is an heavy molecule with 11 atoms. Its structural isomer, 2-aminopropionitrile ($CH_3CH(NH_2)CN$), was studied in a very detailed laboratory survey by Møllendal et al. [1]. It was searched in a deep 3 mm line survey of Sgr B2(N) performed with the IRAM 30 m telescope but, despite a few transitions that could be considered as tentively detected, no clear identification of the molecule could be claimed and a column density upper limit of 1.7×10^{16} cm^{-2} was derived for an assumed source size of 2".

In order to explore the degree of chemical complexity in the ISM, we recently performed the EMoCA survey, a 3 mm spectral line survey of Sgr B2(N) with the Atacama Large Millimeter/submillimeter Array (ALMA) (Belloche et al. [10, 11]). This survey represents an improvement by more than one order of magnitude both in sensitivity and angular resolution compared to our previous IRAM 30 m survey. With this sensitive survey, we revisit the search for 2-aminopropionitrile, and start the search for its structural isomer, 3-aminopropionitrile that first requires an experimental and theoretical study of its rotational spectrum. The analysis of the rotational spectrum of 3-aminopropionitrile is described in Sect. 4. In Sect. 5, we describe the observational details, and the observational results concerning both isomers of aminopropionitrile as well as aminoacetonitrile are reported in Sect 6. These results are discussed in Sect. 7, and we present our conclusions in Sect. 8.

2. Experimental details

The sample was purchased from TCI Europe N.V. and was used without further purification.

The submillimeter-wave spectra of 3-aminopropionitrile were recorded with the Lille spectrometer (150–990 GHz) [12]. The sources are only solid-state devices. The frequency of the Agilent synthesizer (12.5–18.25 GHz) was first multiplied by six and amplified by a Spacek active sextupler providing the output power of +15 dBm in the W-band range (75–110 GHz). This power is sufficiently high to use passive Schottky multipliers (×2, ×3, ×5, ×2×3, ×3×3) from Virginia Diodes Inc. in the next stage of the frequency multiplication chain. As a detector we used an InSb liquid He-cooled bolometer from QMC Instruments Ltd. to improve the sensitivity of the spectrometer; the source was frequency modulated at 10 kHz. The absorption cell was a stainless-steel tube (6 cm diameter, 220 cm long). The sample pressure during measurements was about 1.5 Pa (15 μbar) and the linewidth was limited by Doppler broadening. These measurements were performed at room temperature up to 500 GHz. The measurement accuracy for isolated lines is estimated to be better than 30 kHz up to 500 GHz, determined by the Doppler effect. However, if the lines were blended or had a poor signal-to-noise ratio, they were assigned an uncertainty of 100 or even 200 kHz.

3. Ab initio calculations

Preliminary ab initio calculations were performed employing the Gaussian 09 suite of programs [13]. The structures, dipole moments, energies and vibration-rotation interaction constants (the $\alpha's$) [14] were calculated using density functional theory (DFT) calculations employing Becke's three-parameter hybrid functional [15] and the Lee, Yang and Parr correlation functional (B3LYP) [16] and the Møller & Plesset second order perturbation calculations (MP2) [17]. The 6-311++G(3df, 2pd) wave function augmented with diffuse functions was employed in the B3LYP calculations. The Peterson and Dunnings [18]

correlation-consistent triple-ζ wave function augmented with diffuse functions, aug-cc-pVTZ, was used in the MP2 calculations.

The results include structural optimization as well as harmonic and anharmonic force field computations in order to provide the information about the rotational, quartic and sextic centrifugal distortion constants as well as the low frequency vibrational modes.

Calculations of the electronic energies for all the possible conformations are listed in Table 1. The value of the electronic energy of conformer I is the lowest by less than 0.62 kJ.mol^{-1}: conformation I appears to be more stable than conformation II but the results of MP2/aug-cc-pVTZ calculations are assumed to only be accurate to within 1 kJ.mol^{-1}. Therefore, no valid conclusion can be inferred from this result. Finally, III, IV and V do not need to be considered further because their populations are insignificant under the conditions prevailing in the ISM (see Table 1). This study is thus focused on the first two conformers, denoted I and II and illustrated in Fig. 1. Other conformers are illustrated in Fig. 2.

Table 1: Energy differences between all the possible conformations of 3-aminopropionitrile. The conformers are numbered according to the paper of Braathen et al. [19].

Conformer	I[a]	II	III	IV	V
ΔE (cm^{-1})	0.00	52.23	557.25	264.69	370.25
ΔE (kJ.mol^{-1})	0.00	0.62	6.67	3.16	4.43

MP2/aug-cc-pVTZ ab initio calculations.

[a]Electronic energy of conformer I corrected for zero-point vibrational effect: 595 702.22 kJ.mol^{-1}.

Calculations of the rotational constants, Watson's quartic centrifugal distortion constants as well as the dipole moment components are listed in Table 5 for these two conformers while the calculation results of conformers III, IV and V are tabulated in Table 2. Calculations of the harmonic and anharmonic vibrational frequencies and the vibration-rotation interaction constants (the α's)

Table 2: MP2/aug-cc-pVTZ parameters of spectroscopic interest of conformers III, IV and V of 3-aminopropionitrile.

Conformer	III	IV	V
Rotational constants (MHz)			
A	10914.95	25409.81	24662.82
B	3214.29	2312.38	2295.44
C	2729.30	2191.72	2180.63
Dipole moment (Debye)			
μ_a	4.50	3.94	3.19
μ_b	2.65	0.28	2.25
μ_c	0.38	0.86	0.00

are reported in Tables 3 and 4 for I and II respectively.

4. Analysis of the rotational spectrum

For the analyses of 3-aminopropionitrile, the work of Braathen et al. [19] in the region of 18–32 GHz, was taken as a basis. Due to the presence of different conformations and because of the low value of their first vibrational excited state (107.2 cm^{-1} and 103.8 cm^{-1} for conformer I and II, respectively), 3-aminopropionitrile shows an extremely dense spectrum.

For each conformation of 3-aminopropionitrile, preliminary predictions and fits of rotational spectra were carried out with programs ASROT and ASFIT [20], using the standard rotational Hamiltonian in Watson's A-reduction in I^r representation [21] and using the A-reduction.

For each conformation, the ground-state, the lowest vibrational mode $v_{27} = 1$ and its overtone $v_{27} = 2$ as well as $v_{26} = 1$ were analyzed. However this paper will focus on the study of ground-states for both conformation while excited states will be the subject of a later paper.

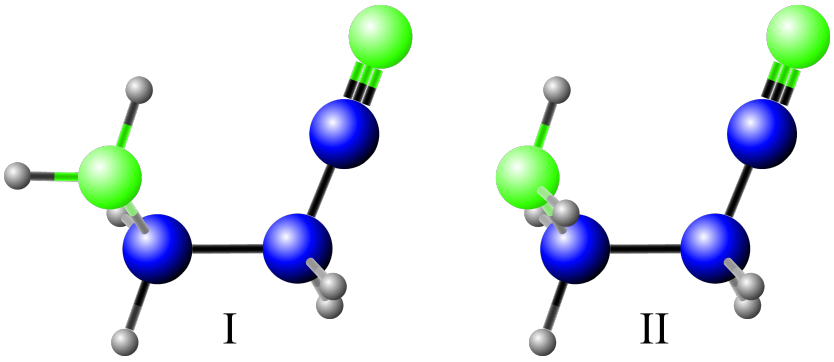

Figure 1: The two C–C–C–N *gauche* conformations of 3-aminopropionitrile ($NH_2CH_2CH_2CN$) denoted I and II.

4.1. Conformation I

From the results of ab initio calculations, conformer I possesses three dipole moment components: a strong μ_a (3.21 D), less strong but significant μ_b (1.97 D) and a weak μ_c (0.77 D). These values, listed in Table 5, are in good agreement with the previous work of Braathen et al. [19] that was estimated based on the bond moment and structure. Therefore, the spectrum contains mainly *a*- and *b*-type lines and the number of transitions collected for each type is summarized in Table 6. This conformer is a near-prolate asymmetric top (Ray's asymmetry parameter, $\kappa = -0.844$).

The spectrum of 3-aminopropionitrile was first analysed in the ground-state using previous parameters and 24 assigned transitions that were used to generate the initial prediction in A-reduction. The assignment of strong ${}^aR$ lines with $K_a = 0$ up to 500 GHz was readily made using these spectroscopic constants. Then, the prediction was improved step by step while adding new identified lines with higher K_a. No *c*-type lines were identified because of the small value of μ_c. 1491 distinct lines (1467 new lines) were assigned and included in the fit, with $0 \leq J \leq 90$ and a K_a value up to 27. The result has a standard deviation of 53 kHz and 20 parameters were determined. The spectroscopic parameters and their uncertainty are presented in Table 7. ${}^bQ$ branches were searched in the spectrum for an identification but no assignment could be made

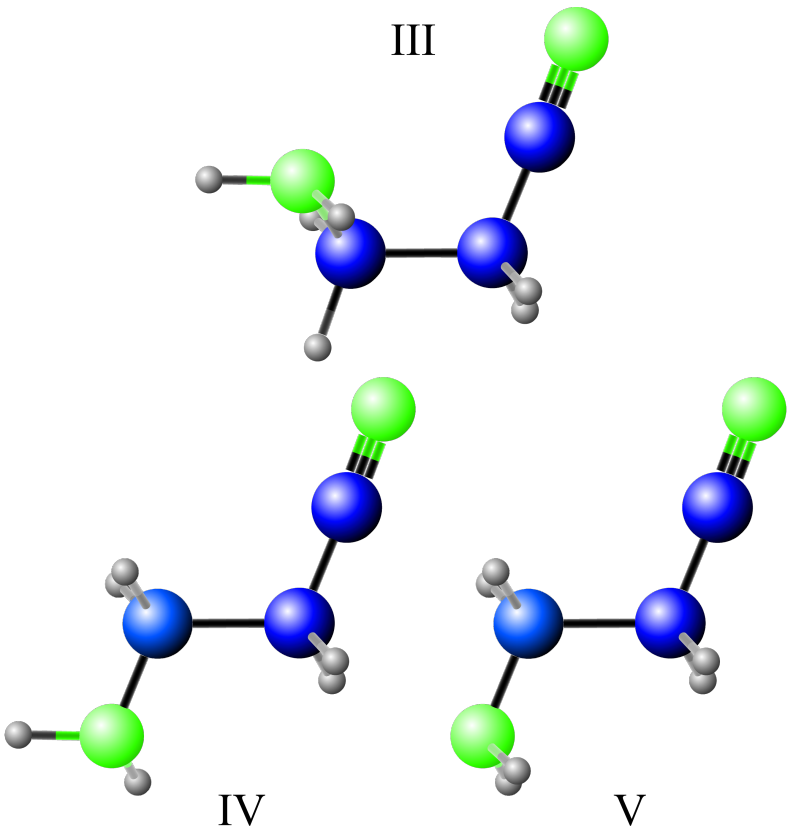

Figure 2: Illustration of conformers III, IV and V which are not analysed in this study.

presumably because of the relative small value of μ_b. In addition, assignment was no longer as simple for every line when the frequency increased, therefore, many lines could not be included in the fit above 400 GHz and varying any of the parameters did not improved the quality of the fit. This effect was encountered many times in the analysis, for both conformers.

Accompanying the ground-state lines, transitions belonging to vibrationally excited states were also observed and assigned. The anharmonic frequencies of the lowest vibrations, listed in Table 3, are 107.2 cm^{-1} (154.2 K) for the first excited state ($v_{27} = 1$) of skeletal C–C torsion, 190.6 cm^{-1} (274.2 K) for the first excited C–N bending mode ($v_{26} = 1$) and 214.0 cm^{-1} (307.9 K) for the

state ($v_{27} = 2$). Only the state $v_{27} = 1$ was previously identified by Braathen et al. [19], therefore, searches were made for the $v_{26} = 1$ and $v_{27} = 2$ states. They were assigned with the help of the vibration-rotation interaction constants (the α's), given in Table 4, as well by the use of the centrifugal distortion constants of the ground-state to build the first frequency predictions. The ground-state dipole moments determined with ab-initio calculations were used for all vibrational state predictions and assignments. The analysis of the $v_{27} = 1$ state was conducted through 500 GHz and 1041 distinct lines were fitted with a standard deviation of 52 kHz. Transitions belonging to the first overtone, $v_{27} = 2$, were readily assigned up to 320 GHz. The fit includes 457 distinct lines and has a standard deviation of 52 kHz. The difficulty encountered during the analysis of conformer I was to deal with the $v_{26} = 1$ vibrational state. Indeed, assignment of the lines with $K_a > 6$ was not straightforward, and at present, it is not clear what is the origin of the perturbation. The analysis of the excited vibrational states is rather beyond the scope of the present study intended to provide accurate frequency predictions for the ground states of the two most stable conformations as the basis for astrophysical observations. Therefore, such analysis will be the subject of a later paper. Here we provide the parameters of vibrationnaly excited states as preliminary results in Supplementary Material Table A.10.

4.2. Conformation II

Conformer II is also not too far from the prolate asymmetric top limit ($\kappa = -0.839$ MHz), its dipole components were calculated to be $\mu_a = 2.16$, $\mu_b = 2.60$ and $\mu_c = 1.06$ D (see Table 5), which indicates that this form should have similar strong a- and b-type spectra and a weak c-type spectrum. These values are nearly equal to those calculated by Braathen et al. [19] but with a b-type spectrum a bit stronger than the a-type one. 1495 distinct lines (1449 new lines) were assigned and included in the fit. The maximum values of the J and K_a quantum numbers for the transitions used in the fit are, respectively, 87 and 24. Nevertheless, four transitions (two distinct lines) from the previous study [19]

were removed from the final fit because of higher residuals (more than 5 σ). The rotational transitions of the second conformer were assigned in a manner similar to the first one, starting with ${}^aR$ lines $K_a = 0$, blended with lines with $K_a = 1$, and improving the fit step by step. Because of the high value of μ_b, many ${}^bQ$ branches were analysed up to 294 GHz, i.e., up to $K_a = 21$. Between 330 and 400 GHz, the spectrum was not recorded. Beyond 400 GHz, the first ${}^bQ$ branch was observed at K_a=29, and some lines were assigned but not included in the fit because of their higher residual (> 5 σ). 37 c-lines were observed and included in the fit resulting in a standard deviation of 53 kHz with 21 parameters. The spectroscopic parameters and their uncertainty are presented in Table 7.

Similary, the same three vibrationally excited states were observed and the analysis was conducted up to 320 GHz for all of them. The assignment was again greatly facilited by the use of Table 4, as well as the use of the centrifugal distortion constants of the ground-state, to build the first frequency predictions. Again, the ground-state dipole moments were used for all vibrational state predictions and assignments. The anharmonic frequencies of the lowest states, given in Table 3, are 103.8 cm^{-1} (149.3 K) and 206.0 cm^{-1} (296.4 K) for $v_{27=1}$ and its overtone, and 186.8 cm^{-1} (268.8 K) for $v_{26} = 1$. For the $v_{27} = 1$ state, the assignments of 830 lines were included in a fit with a standard deviation of 58 kHz. It contains transitions with J and K_a maximum values of 73 and 24, respectively. For $v_{26} = 1$ state, the spectrum was fully characterized up to 320 GHz with the assignment of 589 lines with a J value up to 57 and a K_a value up to 23. 17 free parameters derived a fit with a standard deviation of 53 kHz. Finally, the overtone $v_{27} = 2$ was also observed in the spectrum. Because of the weak intensity of the different transitions of this mode and perturbations, only 153 lines were assigned with maximum values of J and K_a of 55 and 6, respectively. The fit was performed with 8 free and 13 fixed parameters, leading to a standard deviation of 65 kHz. As for conformation I, the investigation of the perturbations in the lowest excited vibrational states of conformation II will we the subject of a separate study. Here the parameters of vibrationnaly excited states are listed as preliminary results in Supplementary Material Table A.11.

4.3. Energy difference between conformers I and II

An estimation of the relative energy from the experimental intensity was performed for conformation I and II. The intensities of 10 lines with close quantum numbers and not too far from each other on the frequency range were compared. A value of 46 ± 11 cm^{-1} was though calculated, which is in good agreement with the listed one in Table 1.

4.4. Predictions

The two new derived sets of spectroscopic constants have permitted to produce predictions in the format of the JPL-CDMS catalog [22] for both conformers in the ground-state up to 500 GHz. Two short examples are provided in Supplementary Material, Table A.12 and Table A.13. Beyond this limit of 500 GHz, it would be hazardous to generate predictions because of strong perturbations between the different states (perturbations which have been noticed during the analysis, see Sect. 4.1). However, the lines that are the most suitable for detection, i.e., the lines with a low K_a, are well fitted. Therefore, they can be used for an astrophysical detection.

4.5. Partition functions

Partition functions were computed taking into account all observed vibrational mode contributions in order to derive column densities which are directly proportional to the partition function. Indeed, low-energy vibrationally excited states around 200 cm^{-1} are populated, even at ISM temperature. As a consequence, the total partition function becomes greatly different from the ground-state one with increasing temperature as illustrated in Table 8. Omitting the vibrational part would underestimate by almost a factor two the column density at 150 K.

Partition functions of the two conformers were calculated using Eq. 1, as used by Widicus Weaver et al. [23] for glycolaldehyde with the same approximations:

$$Q_{\mathrm{Total}} = \sum_{i=0}^{3} e^{-E_i/kT} Q_{i\ \mathrm{ROT}}, \tag{1}$$

where $Q_{i\ \mathrm{ROT}}$ was obtained for each state using the SPCAT program [22]. $i = 0$ stands for the ground-state while $i = 1$, 2 and 3 correspond to the vibrationally excited states analysed in this study. The rotational and vibrational temperatures are assumed to be identical.

Finally, one should take into account contribution of both conformers in the calculation of the partition function by using the following expression:

$$Q_{\mathrm{I+II}} = Q_{\mathrm{I}} + Q_{\mathrm{II}} e^{-\Delta E/kT}, \tag{2}$$

where ΔE is the energy difference between conformers I and II as given in Table 1.

5. Observations and spectral line catalogs

We use the spectral line survey EMoCA performed with the Atacama Large Millimeter/submillimeter Array (ALMA) toward Sgr B2(N). Details about the observational setup and the reduction and modelling of the data are reported in Belloche et al. [11]. In short, the survey covers the frequency range from 84.1 GHz to 114.4 GHz at a median angular resolution of 1.6″. The channel spacing is 488 kHz. The phase center is located at the position with equatorial coordinates $(\alpha, \delta)_{\mathrm{J2000}}$=($17^{\mathrm{h}}47^{\mathrm{m}}19.87^{s}, -28°22'16.0''$), half way between the two hot molecular cores Sgr B2(N1) and Sgr B2(N2). The typical rms noise level is 3 mJy beam^{-1}, or 0.15 K. The size (Full Width at Half Maximum) of the primary beam varies between 69″ at 84 GHz and 51″ at 114 GHz.

In the following section, we model the spectra with Weeds [24], which is part of the GILDAS software[2]. We use the spectroscopic predictions presented in the previous section to model the emission of the two lowest conformers of 3-aminopropionitrile. We also model the emission of aminoacetonitrile and its ^{13}C isotopologs using the spectroscopic predictions available in the Cologne Database for Molecular Spectroscopy [CDMS[3], 25, 26, tags 56507 version 2,

[2]http://www.iram.fr/IRAMFR/GILDAS.
[3]http://www.cdms.de.

57513 version 1, and 57514 version 1]. The ^{12}C entry is mainly based on Motoki et al. [27] and the ^{13}C entries on Kolesnikovà et al. [28]. We also use the CDMS entry 70505 for 2-aminopropionitrile that is based on Møllendal et al. [1].

6. Observational results

We searched for emission lines of the two lowest conformers of 3-aminopropionitrile in the spectrum of the secondary hot core Sgr B2(N2) that has narrower linewidths ($\sim$5 km s^{-1}) and thus a lower level of spectral confusion than Sgr B2(N1). The coordinates of Sgr B2(N2) are $(\alpha, \delta)_{J2000}$=($17^h47^m19.86^s$, $-28°22'13.4''$). The search was done in a systematic way by modeling the expected emission with Weeds under the assumption of local thermodynamic equilibrium (LTE), which is certainly a good approximation given the high densities characterizing the Sgr B2(N2) hot core [$\sim 1.4 \times 10^7$ cm^{-3}, see 29]. The model including all molecules identified so far was used to point out blends and prevent misassignments. We do not detect 3-aminopropionitrile toward Sgr B2(N2). The most stringent constraints are set by the transitions at 93.039 GHz, 95.288 GHz, and 111.502 GHz for conformer I, and at 90.458 GHz, 100.343 GHz, 101.506 GHz, and 111.159 GHz for conformer II.

In order to derive an upper limit to the column densities of both conformers, we first model the emission of aminoacetonitrile, NH_2CH_2CN, which was first detected by Belloche et al. [3] [4] toward Sgr B2(N) with the IRAM 30 m telescope. The molecule is detected toward Sgr B2(N2) in the EMoCA survey too, with 17 features that are clearly detected, that is that have a high signal-to-noise ratio and are not, or only slightly, contaminated by emission from other species (Fig. 3). The fit to the population diagram of aminoacetonitrile shown in Fig. 4 yields a rotational temperature of 108 ± 19 K. This temperature is not well constrained due to a lack of high-energy transitions and maybe also residual contamination of the detected transitions by emission from still unidentified species. Therefore, we adopt a temperature of 150 K, typical of temperatures derived for other species detected in this source [10, 11, 30], and still consistent

within 2σ with the fitted rotational temperature. The size of the aminoacetonitrile emission was derived from Gaussian fits to the integrated intensity maps of its uncontaminated transitions. We obtain a median size of $\sim$0.7″ (FWHM). We measure linewidths of $\sim$6.5 km s^{-1} (FWHM) in the spectrum, and the lines peak at a velocity offset of 0 km s^{-1} with respect to the assumed systemic velocity of the source, 74 km s^{-1}. With these parameters (temperature, source size, linewidth, velocity offset), we fit the detected lines under the LTE assumption. The derived column density is reported in Table 9 and the resulting best-fit synthetic spectrum is shown in Fig. 3. Using the same set of parameters, we also searched for emission of both ^{13}C isotopologs of aminoacetronitrile. None is detected, and upper limits to their column densities are reported in Table 9.

We derive upper limits to the column densities of the two lowest conformers of 3-aminopropionitrile by producing synthetic spectra with the same source size, temperature, linewidth, and velocity offset as for aminoacetonitrile. The resulting upper limits are reported in Table 9, along with an upper limit to the column density of the structural isomer 2-aminopropionitrile that is not detected either.

Table 9 shows that 3-aminopropionitrile is at least 12 times less abundant than aminoacetonitrile, while 2-aminopropionitrile is at least 5 times less abundant than aminoacetonitrile. We also obtain a lower limit of 8 for the ^{12}C/^{13}C isotopic ratio of aminoacetonitrile, which is not very constraining given the typical ratio of 20–25 found for other complex organic molecules in Sgr B2(N2) [11, 30].

7. Discussion

3-Aminopropionitrile contains a longer carbon chain than aminoacetonitrile, with one more carbon atom. We may thus expect a column density ratio [NH_2CH_2CN]/[$NH_2CH_2CH_2CN$] similar to that of pairs of molecules with one carbon atom difference in other families of molecules. The column density ratio between ethyl cyanide and *normal*-propyl cyanide in Sgr B2(N2) is

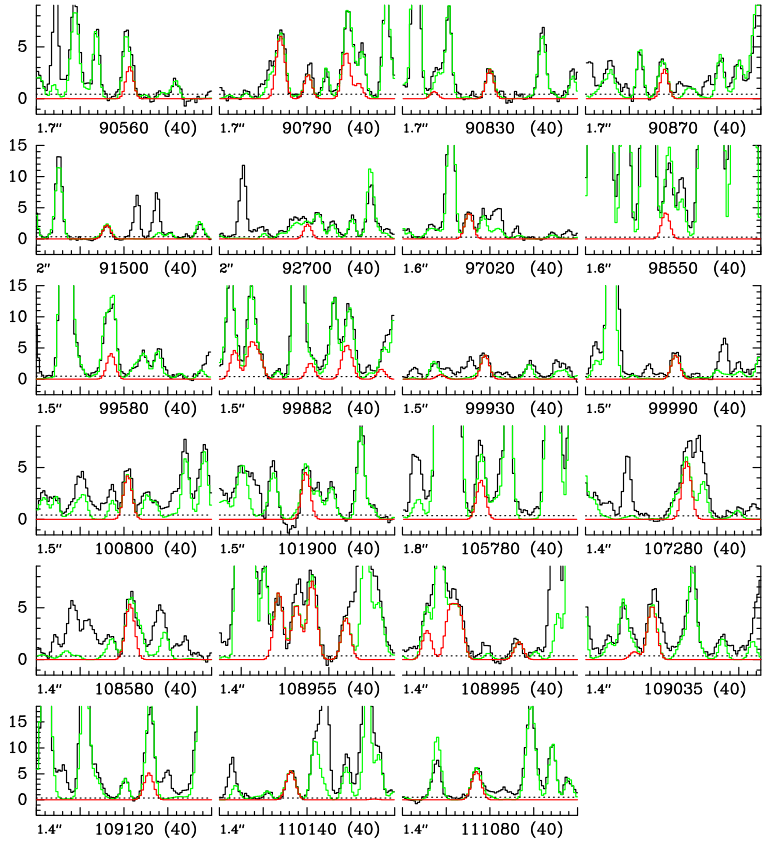

Figure 3: Transitions of NH_2CH_2CN, $v = 0$ covered by our ALMA survey. The best-fit LTE synthetic spectrum of NH_2CH_2CN, $v = 0$ is displayed in red and overlaid on the observed spectrum of Sgr B2(N2) shown in black. The green synthetic spectrum contains the contributions of all molecules identified in our survey so far, including the species shown in red. The central frequency and width are indicated in MHz below each panel. The angular resolution (HPBW) is also indicated. The y-axis is labeled in brightness temperature units (K). The dotted line indicates the 3σ noise level.

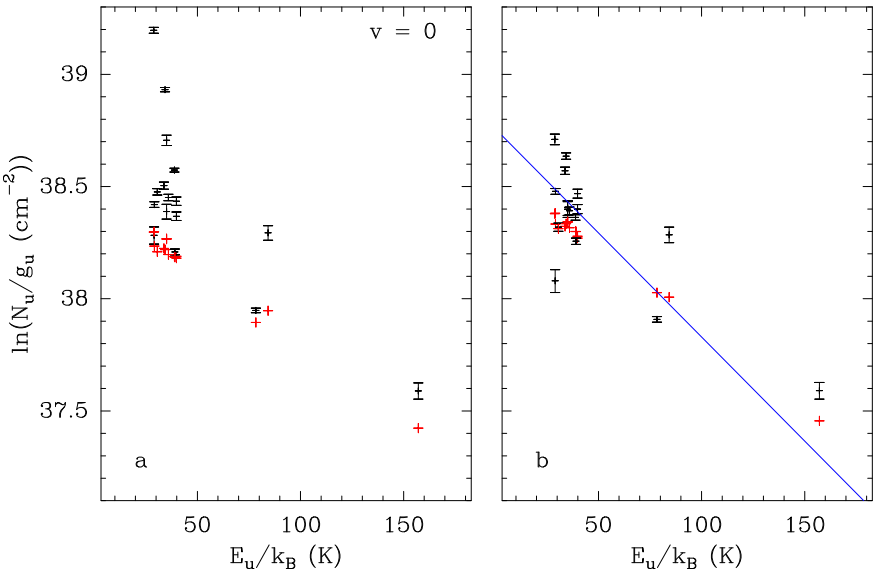

Figure 4: Population diagram of NH_2CH_2CN, $v = 0$ toward Sgr B2(N2). The observed datapoints are shown in black while the synthetic populations are shown in red. No correction is applied in panel **a**. In panel **b**, the optical depth correction has been applied to both the observed and synthetic populations and the contamination by all other species included in the full model has been removed from the observed datapoints. The blue line is a linear fit to the observed populations (in linear-logarithmic space).

[C_2H_5CN]/[n-C_3H_7CN] $\sim$ 34 [10, 11], which is nearly a factor three higher than the lower limit we obtain for [NH_2CH_2CN]/[$NH_2CH_2CH_2CN$]. This suggests that we may have been only by a factor of three short of a detection of 3-aminopropionitrile with the EMoCA survey.

We can also compare our results for 2- and 3-aminopropionitrile, which are structural isomers of each other, to the column density ratio of n-propyl cyanide to its branched, structural isomer, *iso*-propyl cyanide. The ratio [n-C_3H_7CN]/[i-C_3H_7CN] is 2.5 in Sgr B2(N2) [10], so we could expect 2-aminopropionitrile to be 2.5 times less abundant than 3-aminopropionitrile. However, models by Garrod et al. [31] show that the production of both forms of propyl cyanide, and their resultant gas-phase ratios, is dependent on the efficient addition of the CN radical to the unsaturated hydrocarbons C_2H_2, C_2H_4 and C_3H_6 on dust-grains. It is unclear how the equivalent processes involving the addition of CN to amines should behave, nor how dominant they would be in determining the abundances of 2- or 3-aminopropionitrile. The amines are likely to be significantly less abundant than their equivalent hydrocarbons (e.g. CH_3CHNH or CH_2CHNH_2 vs C_3H_6), weakening the influence of such processes. If the formation of aminopropionitrile is instead dependent solely on the direct addition of functional-group radicals, the result would likely be, as per the propyl cyanide models of Belloche et al. [10], an overabundance of the branched form. Our current upper limits for both molecules do not allow to test this hypothesis.

Detecting 3-aminopropionitrile in Sgr B2(N2) will require a sensitivity improvement by a factor three at least. This may be within the range of our on-going Cycle 4 ALMA project which is a follow-up of the EMoCA survey and will provide an improvement in sensitivity and angular resolution by a factor three. The gain in angular resolution will better couple to the expected size of the 3-aminopropionitrile emission if it traces the same region as aminoacetonitrile.

8. Conclusion

Rotational spectra of two conformers of 3-aminopropionitrile were analysed in the laboratory for the ground state and the first three excited vibrational modes up to 500 GHz and 320 GHz, respectively. The two sets of molecular parameters permit to generate accurate predictions for the ground state up to 500 GHz. Total partition functions were also determined taking into account the different vibrational modes observed. Predictions of the rotational spectra of the ground vibrational states of the lowest two 3-aminopropionitrile conformers will be available in the catalog section of the CDMS [26, 32]; line, parameter, and fit files along with further auxiliary files will be available in the catalog archive. Thanks to these frequency predictions, the molecule was searched toward the hot core Sgr B2(N2). We also searched for its structural isomer 2-aminopropionitrile. Neither molecule is detected. The derived upper limits imply that 3- and 2-aminopropionitrile are at least 12 and 5 times less abundant than aminoacetonitrile, respectively. A comparison to ethyl cyanide and n-propyl cyanide detected in this source suggests that an improvement by a factor three in sensitivity may be sufficient to detect 3-aminopropionitrile, which could be within the range of our on-going follow-up project with ALMA.

9. Acknowledgements

This work was supported by the Centre National d'Etudes Spatiales (CNES) and the Action sur Projets de l'INSU, "Physique et Chimie du Milieu Interstellaire". C.R. gratefully acknowledges the ANR-08-BLAN-0225 for a post-doc fellowship. This work has been in part supported by the Deutsche Forschungsgemeinschaft (DFG) through the collaborative research grant SFB 956 "Conditions and Impact of Star Formation", project area B3. This paper makes use of the following ALMA data: ADS/JAO.ALMA#2011.0.00017.S, ADS/JAO.ALMA#2012.1.00012.S. ALMA is a partnership of ESO (representing its member states), NSF (USA), and NINS (Japan), together with NRC (Canada), NSC and ASIAA (Taiwan), and KASI (Republic of Korea), in cooperation with the Republic of Chile. The

Joint ALMA Observatory is operated by ESO, AUI/NRAO, and NAOJ. The interferometric data are available in the ALMA archive at https://almascience.eso.org/aq/.

Appendix A. Supplementary Material

References

[1] H. Møllendal, L. Margulès, A. Belloche, R. Motiyenko, A. Konovalov, K. Menten, J.-C. Guillemin, Rotational spectrum of a chiral amino acid precursor, 2-aminopropionitrile, and searches for it in Sagittarius B2 (N), Astronomy & Astrophysics 538 (2012) A51. doi:10.1051/0004-6361/201116838.

[2] C. Richard, L. Margulès, R. A. Motiyenko, J.-C. Guillemin, Analysis of the terahertz rotational spectrum of the three mono-13C ethyl cyanides (13C–CH3CH2CN), Astronomy & Astrophysics 543 (2012) A135. doi:10.1051/0004-6361/201219713.

[3] A. Belloche, K. Menten, C. Comito, H. Müller, P. Schilke, J. Ott, S. Thorwirth, C. Hieret, Detection of amino acetonitrile in Sgr B2 (N), Astronomy & Astrophysics 482 (1) (2008) 179–196. doi:10.1051/0004-6361:20079203.

[4] A. Belloche, K. Menten, C. Comito, H. Müller, P. Schilke, J. Ott, S. Thorwirth, C. Hieret, Detection of amino acetonitrile in Sgr B2 (N) (Erratum), Astronomy & Astrophysics 492 (3) (2008) 769–773. doi:10.1051/0004-6361:20079203e.

[5] A. Belloche, R. Garrod, H. Müller, K. Menten, C. Comito, P. Schilke, Increased complexity in interstellar chemistry: detection and chemical modeling of ethyl formate and n-propyl cyanide in sagittarius B2 (N), Astronomy & Astrophysics 499 (1) (2009) 215–232. doi:10.1051/0004-6361/200811550.

[6] M. Werner, K. Uchida, K. Sellgren, M. Marengo, K. Gordon, P. Morris, J. Houck, J. Stansberry, New infrared emission features and spectral vari-

ations in NGC 7023, The Astrophysical Journal Supplement Series 154 (1) (2004) 309.

[7] K. Sellgren, M. W. Werner, J. G. Ingalls, J. Smith, T. Carleton, C. Joblin, C60 in reflection nebulae, The Astrophysical Journal Letters 722 (1) (2010) L54. doi:10.1088/2041-8205/722/1/L54.

[8] J. Cami, J. Bernard-Salas, E. Peeters, S. E. Malek, Detection of C60 and C70 in a young planetary nebula, Science 329 (5996) (2010) 1180–1182. doi:10.1126/science.1192035.

[9] B. Foing, P. Ehrenfreund, Detection of two interstellar absorption bands coincident with spectral features of C60+, Nature 369 (6478) (1994) 296–298.

[10] A. Belloche, R. T. Garrod, H. S. Müller, K. M. Menten, Detection of a branched alkyl molecule in the interstellar medium: iso-propyl cyanide, Science 345 (6204) (2014) 1584–1587. doi:10.1126/science.1256678.

[11] A. Belloche, H. Müller, R. Garrod, K. Menten, Exploring molecular complexity with ALMA (EMoCA): Deuterated complex organic molecules in Sagittarius B2 (N2), Astronomy & Astrophysics 587 (2016) A91. doi:10.1051/0004-6361/201527268.

[12] R. Motiyenko, L. Margulès, E. Alekseev, J.-C. Guillemin, J. Demaison, Centrifugal distortion analysis of the rotational spectrum of aziridine: Comparison of different Hamiltonians, Journal of Molecular Spectroscopy 264 (2) (2010) 94–99. doi:10.1016/j.jms.2010.09.007.

[13] M. Frisch, G. Trucks, H. Schlegel, G. Scuseria, M. Robb, J. Cheeseman, G. Scalmani, V. Barone, B. Mennucci, G. Petersson, et al., Gaussian 09, revision D. 01 (2009).

[14] W. Gordy, R. L. Cook, Microwave molecular spectra, Wiley (New-York), 1984.

[15] A. D. Becke, Density-functional exchange-energy approximation with correct asymptotic behavior, Physical review A 38 (6) (1988) 3098. doi:10.1103/PhysRevA.38.3098.

[16] C. Lee, W. Yang, R. G. Parr, Development of the Colle-Salvetti correlation-energy formula into a functional of the electron density, Physical review B 37 (2) (1988) 785. doi:10.1103/PhysRevB.37.785.

[17] C. Møller, M. S. Plesset, Note on an approximation treatment for many-electron systems, Physical Review 46 (7) (1934) 618. doi:10.1103/PhysRev.46.618.

[18] K. A. Peterson, T. H. Dunning Jr, Accurate correlation consistent basis sets for molecular core–valence correlation effects: The second row atoms Al–Ar, and the first row atoms B–Ne revisited, The Journal of chemical physics 117 (23) (2002) 10548–10560. doi:10.1063/1.1520138.

[19] O.-A. Braathen, K.-M. Marstokk, H. Mollendal, Microwave spectrum, conformational equilibrium, intramolecular hydrogen bonding and centrifugal distortion of 3-aminopropionitrile, Acta Chem. Scand. A 37 (6) (1983) 493–501. doi:10.3891/acta.chem.scand.37a-0493.

[20] Z. Kisiel, PROSPE–Programs for ROtational SPEctroscopy (2001).

[21] J. K. Watson, Aspects of quartic and sextic centrifugal effects on rotational energy levels, Vibrational spectra and structure 6 (1977) 1–89.

[22] H. M. Pickett, The fitting and prediction of vibration-rotation spectra with spin interactions, Journal of Molecular Spectroscopy 148 (2) (1991) 371–377. doi:10.1016/0022-2852(91)90393-O.

[23] S. L. W. Weaver, R. A. Butler, B. J. Drouin, D. T. Petkie, K. A. Dyl, F. C. De Lucia, G. A. Blake, Millimeter-wave and vibrational state assignments for the rotational spectrum of glycolaldehyde, The Astrophysical Journal Supplement Series 158 (2) (2005) 188.

[24] S. Maret, P. Hily-Blant, J. Pety, S. Bardeau, E. Reynier, Weeds: a CLASS extension for the analysis of millimeter and sub-millimeter spectral surveys, Astronomy & Astrophysics 526 (2011) A47. doi:10.1051/0004-6361/201015487.

[25] H. Müller, S. Thorwirth, D. Roth, G. Winnewisser, The Cologne database for molecular spectroscopy, CDMS, Astronomy & Astrophysics 370 (3) (2001) L49–L52. doi:10.1051/0004-6361:20010367.

[26] H. S. Müller, F. Schlöder, J. Stutzki, G. Winnewisser, The Cologne Database for Molecular Spectroscopy, CDMS: a useful tool for astronomers and spectroscopists, Journal of Molecular Structure 742 (1) (2005) 215–227. doi:10.1016/j.molstruc.2005.01.027.

[27] Y. Motoki, Y. Tsunoda, H. Ozeki, K. Kobayashi, Submillimeter-Wave Spectrum of Aminoacetonitrile and Its Deuterated Isotopologues, Possible Precursors of the Simplest Amino Acid Glycine, The Astrophysical Journal Supplement Series 209 (2) (2013) 23. doi:10.1088/0067-0049/209/2/23.

[28] L. Kolesniková, E. Alonso, S. Mata, J. Alonso, Rotational Spectra in 29 Vibrationally Excited States of Interstellar Aminoacetonitrile, The Astrophysical Journal Supplement Series 229 (2) (2017) 26. doi:10.3847/1538-4365/aa5d13.

[29] M. Bonfand, A. Belloche, K. Menten, R. Garrod, H. Müller, Exploring molecular complexity with ALMA (EMoCA): Detection of three new hot cores in Sagittarius B2(N), Astronomy & Astrophysics in press.

[30] H. S. Müller, A. Belloche, L.-H. Xu, R. M. Lees, R. T. Garrod, A. Walters, J. van Wijngaarden, F. Lewen, S. Schlemmer, K. M. Menten, Exploring molecular complexity with ALMA (EMoCA): Alkanethiols and alkanols in Sagittarius B2 (N2), Astronomy & Astrophysics 587 (2016) A92. doi:10.1051/0004-6361/201527470.

[31] R. Garrod, A. Belloche, H. Müller, K. Menten, Exploring molecular complexity with ALMA (EMoCA): Simulations of branched carbon-chain chemistry in Sgr B2 (N), Astronomy & Astrophysics 601 (2017) A48.

[32] C. P. Endres, S. Schlemmer, P. Schilke, J. Stutzki, H. S. Müller, The Cologne Database for Molecular Spectroscopy, CDMS, in the Virtual Atomic and Molecular Data Centre, VAMDC, Journal of Molecular Spectroscopy 327 (2016) 95–104.

Table 3: The B3LYP/6-311G(3df, 2pd) harmonic and anharmonic vibrational fundamentals of 3-aminopropionitrile (in cm^{-1}).

Conformer	I		II	
Mode	E(harm.)	E(anharm.)	E(harm.)	E(anharm.)
1	3584.1	3418.3	3585.9	3417.1
2	3502.8	3336.5	3504.5	3387.7
3	3088.9	2944.3	3087.7	2948.3
4	3070.2	2972.0	3069.1	2926.2
5	3045.6	2951.9	3042.8	2908.7
6	2972.6	2854.3	3032.3	2945.1
7	2349.7	2320.0	2348.4	2316.3
8	1660.1	1755.1	1663.3	1660.6
9	1514.3	1743.3	1494.2	1484.4
10	1462.4	1441.0	1468.3	1445.3
11	1420.8	1398.6	1392.0	1357.0
12	1354.5	1321.7	1390.8	1358.1
13	1338.1	1303.5	1337.1	1303.8
14	1239.0	1211.1	1249.8	1220.4
15	1171.5	1146.6	1170.7	1147.6
16	1101.2	1069.5	1108.2	1075.3
17	1068.9	1037.7	1000.3	971.5
18	968.3	948.1	963.6	949.6
19	873.2	852.3	847.3	827.9
20	822.4	905.6	829.1	781.7
21	814.7	798.6	782.7	741.7
22	577.5	569.9	578.2	574.3
23	398.0	394.1	388.3	383.8
24	382.2	381.7	375.0	372.3
25	262.1	246.7	309.6	293.0
27(2)	222.7	214.0	221.0	206.1
26	195.2	190.6	190.5	186.8
27	111.4	107.2	110.5	103.8

Table 4: B3LYP/6-311++G(3df, 2pd) vibration-rotation α matrix of 3-aminopropionitrile (MHz).

Component	a_{calc}	a_{obs}	b_{calc}	b_{obs}	c_{calc}	c_{obs}
			Conformer I			
$Q(27=2)$	−178.06	−175.79	19.82	27.07	13.40	16.39
$Q(26)$	−13.13	−3.79	−0.12	−0.39	−0.15	0.14
$Q(27)$	−89.03	−86.46	9.91	13.43	6.70	8.22
			Conformer II			
$Q(27=2)$	−141.94	−150.52	11.44	19.79	9.72	13.60
$Q(26)$	−1.74	−4.10	−5.85	−6.33	−2.19	−2.35
$Q(27)$	−70.97	−72.28	5.72	9.72	4.86	6.81

Table 5: MP2/aug-cc-pVTZ and B3LYP/6-311G(3df, 2pd) parameters of spectroscopic interest of the first two conformers of 3-aminopropionitrile in A-reduction.

Conformer	I	II
Rotational constants (MHz)[a]		
A	10409.86	10196.48
B	3454.22	3413.92
C	2819.20	2787.81
Quartic centrifugal distortion constants (kHz)[a]		
Δ_J	4.21	4.17
Δ_{JK}	−23.34	−23.54
Δ_K	63.90	63.04
δ_J	1.30	1.28
δ_K	8.69	7.93
Sextic centrifugal distortion constants (Hz)[b]		
Φ_J	0.0039	0.0066
Φ_{JK}	−0.02250	−0.0448
Φ_{KJ}	−0.4138	−0.3142
Φ_K	1.8822	1.4756
ϕ_J	0.00193	0.0031
ϕ_{JK}	−0.1048	−0.0825
ϕ_K	0.6949	0.7217
Dipole moment (Debye)[a]		
μ_a	3.21	2.16
μ_b	1.97	2.60
μ_c	0.77	1.06

[a] MP2/aug-cc-pVTZ

[b] B3LYP/6-311G(3df, 2pd)

Table 6: Number and type of transitions assigned in the fit of 3-aminopropionitrile.

Conformer	*a*-transitions	*b*-transitions	*c*-transitions	Total
I				
g.s.	1296	551	0	1847
$v_{27} = 1$	1038	270	0	1308
$v_{26} = 1$	137	111	0	248
$v_{27} = 2$	492	117	0	609
II				
g.s.	787	1023	37	1847
$v_{27} = 1$	540	490	4	1034
$v_{26} = 1$	449	321	0	770
$v_{27} = 2$	138	157	0	295
				7958

Table 7: Spectroscopic constants of the ground-vibrational states for conformer I and II, A-reduction, of 3-aminopropionitrile.

Parameters	Conformer I	Conformer II
A (MHz)	10526.53626(68)	10281.32531(59)
B (MHz)	3387.38499(20)	3367.74302(13)
C (MHz)	2781.57456(17)	2761.07458(13)
Δ_J (kHz)	4.055304(72)	4.014297(60)
Δ_{JK} (kHz)	−23.70723(69)	−23.40219(63)
Δ_K (kHz)	69.5113(30)	66.2287(25)
δ_J (kHz)	1.248175(46)	1.235986(23)
δ_K (kHz)	9.1603(18)	8.2744(14)
Φ_J (Hz)	0.007127(16)	0.008794(12)
Φ_{JK} (Hz)	0.06803(30)	0.04139(76)
Φ_{KJ} (Hz)	−0.7792(14)	−0.7721(32)
Φ_K (Hz)	2.2983(42)	1.9643(34)
ϕ_J (Hz)	0.0033777(98)	0.0042348(29)
ϕ_{JK} (Hz)	−0.04075(56	−0.02875(53))
ϕ_K (Hz)	1.0149(31)	0.755(11)
L_J (mHz)	0.0000249(13)	0.00001731(95)
L_{JJK} (mHz)	−0.000174(19)	0.001296(93)
L_{JK} (mHz)	−0.01786(26)	−0.00872(40)
L_{KKJ} (mHz)		0.0903(25)
l_J (mHz)	0.00001238(70)	
l_{JK} (mHz)	0.000576(46)	0.000723(46)
l_{KJ} (mHz)		0.0281(14)
Number of lines	1492	1495
Number of free parameters	20	21
Frequency max (GHz)	500	500
J(Max), K_a(Max)	90, 27	87, 24
Standard deviation (kHz)	53	53
Weighted deviation	0.93	0.88

Numbers in parentheses are one standard deviation in the same units as the last digit.

Table 8: Partition functions of 3-aminopropionitrile for conformations I and II. The total partition function is compared with the ground-state contribution.

	Conformation I		Conformation II	
T (K)	$Q_{\mathrm{Ground-state}}$	Q_{Total}	$Q_{\mathrm{Ground-state}}$	Q_{Total}
300.000	79 315.53	186 981.54	80 601.10	192 327.96
225.000	54 740.40	112 371.04	55 687.11	116 055.18
150.000	30 905.45	50 877.62	31 467.92	52 676.94
75.000	11 015.11	12 889.06	11 219.37	13 276.57
37.500	3894.42	3961.76	3966.65	4045.07
18.750	1378.05	1378.41	1403.60	1404.08
9.375	488.28	488.28	497.32	497.32

The vibrational part includes the contribution of the excited vibrational states: $v_{27} = 1$, $v_{26} = 1$ and $v_{27} = 2$.

Table 9: Parameters of our best-fit LTE model (or upper limit) of aminoacetonitrile, its ^{13}C isotopologs, and 2- and 3-aminopropionitrile toward Sgr B2(N2).

Molecule	Status[a]	$N_{\rm det}^b$	Size[c]	$T_{\rm rot}^d$	N^e	C^f	ΔV^g	$V_{\rm off}^h$	$\frac{N_{\rm AAN}}{N}^i$
			($''$)	(K)	(cm^{-2})		(km s^{-1})	(km s^{-1})	
NH_2CH_2CN	d	17	0.7	150	9.7 (16)	1.27	6.5	0.0	1
$NH_2{}^{13}CH_2CN$	n	0	0.7	150	$<$ 1.3 (16)	1.27	6.5	0.0	$>$ 8
$NH_2CH_2{}^{13}CN$	n	0	0.7	150	$<$ 1.1 (16)	1.27	6.5	0.0	$>$ 8
$CH_3CH(NH_2)CN$	n	0	0.7	150	$<$ 1.9 (16)	1.48	6.5	0.0	$>$ 5
$NH_2CH_2CH_2CN$, conf. I	n	0	0.7	150	$<$ 8.1 (15)	1.63	6.5	0.0	$>$ 12
$NH_2CH_2CH_2CN$, conf. II	n	0	0.7	150	$<$ 1.3 (16)	1.00	6.5	0.0	$>$ 7

[a]d: detection, n: non-detection. [b]Number of detected lines. Here, one line of a given species may mean a group of transitions of that species that are blended together. [c]Source diameter ($FWHM$). [d]Rotational temperature. [e]Total column density of the molecule. X (Y) means $X \times 10^Y$. [f]Correction factor that was applied to the column density to account for the contribution of vibrationally excited states in the cases where this contribution was not included in the partition function of the spectroscopic predictions. The correction for conformer I of $NH_2CH_2CH_2CN$ takes into account the contribution of conformer II to the global partition function of the molecule. For conformer II, we did not apply any correction and the column density upper limit corresponds to conformer II considered as an independent species. [g]Linewidth ($FWHM$). [h]Velocity offset with respect to the assumed systemic velocity of Sgr B2(N2) $V_{\rm lsr}$ = 74 km s^{-1}. [i]Column density ratio, with $N_{\rm AAN}$ the column density of aminoacetonitrile.

Table A.10: Spectroscopic constants of the first vibrational excited states of conformer I, A-reduction, of 3-aminopropionitrile.

Parameters	$v_{27} = 1$	$v_{26} = 1$	$v_{27} = 2$
Energy (cm^{-1})[a]	107.2	190.6	214.0
A (MHz)	10612.9923(16)	10530.61(44)	10702.319(18)
B (MHz)	3373.94868(22)	3387.726(33)	3360.31475(72)
C (MHz)	2773.35210(24)	2781.41237(51)	2765.17597(52)
Δ_J (kHz)	3.963342(52)	4.0913(51)	3.88598(25)
Δ_{JK} (kHz)	−24.13057(91)	−23.43(24)	−24.6813(33)
Δ_K (kHz)	74.3020(94)	69.5113	79.40(17)
δ_J (kHz)	1.218993(53)	1.2632(25)	1.19535(16)
δ_K (kHz)	9.5297(22)	9.527(58)	9.9753(90)
Φ_J (Hz)	0.0061201(60)	0.007044(39)	0.005083(67)
Φ_{JK} (Hz)	0.07980(29)	0.06803	0.0890(40)
Φ_{KJ} (Hz)	−0.8634(20)	−0.7792	−0.970(19)
Φ_K (Hz)	2.859(16)	2.2983	
ϕ_J (Hz)	0.0028557(94)	0.0033777	0.002360(36)
ϕ_{JK} (Hz)	−0.05707(53)	−0.04075	−0.0692(26)
ϕ_K (Hz)	1.0977(40)	1.0149	1.103(76)
L_J (mHz)	0.0000249	0.0000249	0.0000249
L_{JJK} (mHz)	−0.000174	−0.000174	−0.000174
L_{JK} (mHz)	−0.02225(38)	−0.01786	−0.01786
l_J (mHz)	0.00001296(57)	0.00001238	0.00001238
l_{JK} (mHz)	0.000756(36)	0.000576	0.000576
Number of lines	1041	118	457
Number of free parameters	18	8	14
Frequency max (GHz)	500	320	320
J(Max), K_a(Max)	90, 26	55, 6	57, 15
Standard deviation (kHz)	52	38	52
Weighted deviation	0.94	0.61	0.89

Numbers in parentheses are one standard deviation in the same units as the last digit.
[a]Ab initio values calculated from the anharmonic force field at the level B3LYP/6-311++G(3df, 2pd).

Table A.11: Spectroscopic constants of the first vibrational excited states of conformer II, A-reduction, of 3-aminopropionitrile.

Parameters	$v_{27} = 1$	$v_{26} = 1$	$v_{27} = 2$
Energy (cm^{-1})[a]	103.8	186.8	206.0
A (MHz)	10353.6220(12)	10285.4203(11)	10431.23(30)
B (MHz)	3358.02549(41)	3374.07436(58)	3348.076(22)
C (MHz)	2754.26197(37)	2763.42345(40)	2747.47355(69)
Δ_J (kHz)	3.92665(22)	4.04258(26)	3.8337(38)
Δ_{JK} (kHz)	−23.6070(15)	−23.2395(14)	−21.97(18)
Δ_K (kHz)	70.0218(66)	65.4302(65)	66.2287
δ_J (kHz)	1.20927(13)	1.25296(16)	1.1792(18)
δ_K (kHz)	8.5824(67)	8.4887(74)	9.784(47)
Φ_J (Hz)	0.008622(64)	0.008728(74)	0.008744(51)
Φ_{JK} (Hz)	0.0897(19)	0.0476(22)	0.04139
Φ_{KJ} (Hz)	−0.8789(84)	−0.7998(88)	−0.7721
Φ_K (Hz)	2.267(10)	2.007(11)	1.9643
ϕ_J (Hz)	0.004055(34)	0.004186(40)	0.0042348
ϕ_{JK} (Hz)	−0.0354(22)	−0.0328(24)	−0.02875
ϕ_K (Hz)	1.009(35)	0.822(42)	0.755
L_J (mHz)	0.00001731	0.00001731	0.00001731
L_{JJK} (mHz)	−0.006082(76)	0.001296	0.001296
L_{JK} (mHz)	−0.00872	−0.00872	−0.00872
L_{KKJ} (mHz)	0.0874(69)	0.0903	0.0903
l_{JK} (mHz)	0.000723	0.000723	0.000723
l_{KJ} (mHz)	0.0281	0.0281	0.0281
Number of lines	830	589	153
Number of free parameters	17	15	8
Frequency max (GHz)	320	320	320
J(Max), K_a(Max)	73, 24	57, 23	55, 6
Standard deviation (kHz)	58	53	65
Weighted deviation	1.02	0.92	1.00

Numbers in parentheses are one standard deviation in the same units as the last digit.
[a]Ab initio values calculated from the anharmonic force field at the level B3LYP/6-311++G(3df, 2pd).

Table A.12: Predicted transition frequencies of 3-aminopropionitrile in the ground-vibrational state for conformation I up to 500 GHz. Data are available in their entirety as supplementary material of this journal.

Frequency (MHz)	Error[a] (MHz)	LGINT[b] (nm^2·MHz)	J'	K'_a	K'_c	J''	K''_a	K''_c
10138.2828	0.0068	-6.9433	33	7	26	33	7	27
10140.6671	0.0075	-6.9335	23	5	18	23	5	19
10321.4242	0.0072	-6.9132	28	6	22	28	6	23
10913.6970	0.0014	-6.8366	4	1	3	4	0	4
11728.8306	0.0070	-6.9491	14	3	11	14	3	12
11732.1497	0.0003	-6.6995	2	1	2	1	1	1
12276.3042	0.0100	-6.9076	44	9	35	44	9	36
12300.8602	0.0003	-6.5335	2	0	2	1	0	1
12943.6177	0.0004	-6.6142	2	1	1	1	1	0
12951.0673	0.0022	-6.6542	5	1	4	5	0	5
13163.9240	0.0087	-6.7900	19	4	15	19	4	16
13219.4278	0.0088	-6.7952	39	8	31	39	8	32
13864.2371	0.0085	-6.7224	34	7	27	34	7	28
13925.9147	0.0093	-6.7115	24	5	19	24	5	20
14128.1997	0.0089	-6.6925	29	6	23	29	6	24
14285.4874	0.0036	-6.9862	32	12	21	31	13	18
14285.4973	0.0036	-6.9862	32	12	20	31	13	19
14947.0224	0.0143	-6.8519	50	10	40	50	10	41
15177.8391	0.0082	-6.9619	28	5	24	28	4	24
15422.2204	0.0045	-6.8928	25	9	17	24	10	14

This table was computed with the SPCAT program [22].

[a]Estimated or experimental error of frequency. [b]Base 10 logarithm of the integrated intensity in units of nm^2·MHz at 300 K.

Table A.13: Predicted transition frequencies of 3-aminopropionitrile in the ground-vibrational state for conformation I up to 500 GHz. Data are available in their entirety as supplementary material of this journal.

Frequency (MHz)	Error[a] (MHz)	LGINT[b] (nm^2·MHz)	J'	K'_a	K'_c	J''	K''_a	K''_c
9202.1164	0.0006	-6.8669	3	1	2	3	0	3
9277.4880	0.0040	-6.9512	23	4	20	23	3	20
10170.2270	0.0044	-6.8702	29	5	25	29	4	25
10348.3192	0.0034	-6.9492	16	3	14	16	2	14
10707.1807	0.0009	-6.6694	4	1	3	4	0	4
10840.1020	0.0044	-6.8425	35	6	30	35	5	30
11390.2357	0.0048	-6.8530	41	7	35	41	6	35
11905.4946	0.0064	-6.8919	47	8	40	47	7	40
11996.4622	0.0046	-6.7735	22	4	19	22	3	19
12219.3203	0.0003	-6.8488	2	0	2	1	0	1
12286.9192	0.0041	-6.9759	17	6	12	16	7	9
12337.7625	0.0042	-6.9723	17	6	11	16	7	10
12337.8251	0.0039	-6.9254	24	9	16	23	10	13
12338.4659	0.0039	-6.9253	24	9	15	23	10	14
12339.0906	0.0032	-6.9397	31	12	20	30	13	17
12339.0972	0.0032	-6.9397	31	12	19	30	13	18
12459.0153	0.0094	-6.9522	53	9	45	53	8	45
12761.6173	0.0013	-6.4849	5	1	4	5	0	5
12864.1961	0.0003	-6.9291	2	1	1	1	1	0
12956.6862	0.0036	-6.8148	15	3	13	15	2	13

This table was computed with the SPCAT program [22].

[a]Estimated or experimental error of frequency. [b]Base 10 logarithm of the integrated intensity in units of nm^2·MHz at 300 K.